

Magnetic Suboxides as a Source of Two-Level System Losses in Superconducting Niobium

D. Bafia,^{1,*} A. Grassellino,¹ and A. Romanenko¹

¹*Fermi National Accelerator Laboratory, Batavia, Illinois 60510, USA*

(Dated: August 29, 2022)

We identify one potential source of quantum decoherence in three-dimensional superconducting radio-frequency (SRF) resonators and two-dimensional transmon qubits that utilize oxidized niobium: magnetic suboxides which drive two-level system (TLS) losses. By probing the effect of sequential *in situ* vacuum baking treatments on the RF performance of bulk Nb SRF resonators and on the oxide structure of a representative Nb sample within a time-of-flight secondary ion mass spectrometer (TOF-SIMS), we find a non-monotonic evolution of cavity quality factor Q_0 which correlates with the interplay of TLS-hosting magnetic suboxide generation and oxide dissolution. We localize this effect to the oxide itself and present the non-role of diffused interstitial oxygen in the underlying Nb by regrowing a new oxide *via* chemistry and wet oxidation which reveals a mitigation of aggravated TLS losses.

I. INTRODUCTION

The realization of a computationally useful superconducting quantum computer requires the maximization of quantum coherence lifetimes to unlock quantum memory, high-fidelity gate operations, and better entanglement among qubits [1]. In superconducting systems, quantum coherence is limited by dissipative decay channels present in both the linear resonator and the transmon qubit that contains the nonlinear Josephson junction necessary to create uniquely addressable energy levels. Current decoherence candidates include quasi-particles [2, 3], radiation-induced losses [4, 5], and dielectric losses such as two-level systems (TLS) [6], to name a few. Dielectric loss arises from each material and interface used in the construction of superconducting qubits and dictates the total decay rate of the system according to

$$\Gamma_1 = \frac{1}{T_1} = \frac{\omega}{Q_0} = \omega \sum_i \frac{F_i}{Q_i} + \Gamma_0, \quad (1)$$

where T_1 is the photon lifetime, ω is angular frequency, Q_0 is the quality factor, F_i and Q_i are the filling and quality factors of the i^{th} loss channel, and Γ_0 captures losses driven by non-dielectric mechanisms [7, 8]. The quality factor is inversely related to the dielectric loss tangent $Q_i = 1/\tan\delta_i$. As a result, decay rate minimization requires the mitigation of every loss channel down to tolerable levels. While straightforward for a single interface, this task is difficult in complex multi-layer systems like those used in modern qubit fabrication designs. Many such designs utilize thin films of aluminum and niobium atop dielectric or semiconducting substrates, leading to multiple potentially deleterious materials and interfaces.

Recent work on three-dimensional (3-D) niobium superconducting radio-frequency (SRF) resonators in the

low GHz frequency range has highlighted the amorphous native niobium oxide as a dramatic source of TLS loss, implying an inherent limitation in qubits fabricated with oxidized niobium [9, 10]. By removing the native niobium oxide *via in situ* vacuum baking at 340-450 °C for several hours, a ten-fold improvement in quality factor Q_0 was observed, demonstrating intra-resonator photon lifetimes of $T_1 \approx 2$ s, a 200-fold increase over the previous state-of-the-art [11]. By fitting temperature dependent Q_0 data of bulk niobium resonators with the standard TLS model [12, 13], Romanenko *et al.* found the dielectric loss tangent of the native niobium oxide at 5 GHz to be $\delta_0 = 0.08$. This value is in agreement with values obtained from niobium-on-silicon lumped element resonators post sequential oxidation [14] and niobium-on-silicon coplanar-waveguides post sequential etching [15]. This consistency between dramatically different architectures demonstrates that observations of the Nb-air interface made in simplified, single interface systems such as 3-D Nb SRF resonators are directly translatable to more complex systems such as those used in transmon qubits, allowing for a one-to-one correspondence between thin film and bulk material measurements.

While there exists an empirical mitigation strategy to minimize their deleterious effect in superconducting quantum systems, the precise origin and nature of the TLS losses within the niobium oxide is not yet fully understood. A complete picture of the underlying mechanisms would aid in the further development of mitigation strategies that may instead be stable to air. There exist a few possible origins for these TLS losses. Oxygen vacancies within the amorphous oxide have the potential of creating magnetic impurities [16, 17] and driving impedance, as supported by X-ray absorption spectroscopy studies [18] and density functional theory calculations [18, 19]. These oxygen vacancies may serve as OH tunneling sites [20]. Another possibility stems from the conducting or magnetic nature of the NbO_x oxides [10]. Here, we present results that support the role of the latter in driving TLS losses in oxidized niobium.

* dbafia@fnal.gov

One avenue for identifying the origins of loss in the amorphous native Nb oxide is by studying its evolution with *in situ* baking, allowing for the investigation of the role of various oxides on Q_0 . There exists extensive literature on this topic as it is relevant for high Q_0 and high electric field applications of Nb SRF resonators in particle accelerators. It is well known that native niobium oxides exist in a graded structure composed of Nb_2O_5 (insulator [21]), NbO_2 (semiconductor [22]), NbO (metallic [23]), and the metal substrate [21, 24]. *In situ* vacuum baking dissolves the dominant pentoxide and grows the suboxides, reducing according to $\text{Nb}_2\text{O}_5 \rightarrow \text{NbO}_2 \rightarrow \text{NbO}$ [24–27]. Ma *et al.* showed that *in situ* vacuum baking at 150°C for 40 hours reduced the pentoxide to NbO_2 ; continued baking at 280°C for 8 hours showed further reduction to metallic Nb_xO ($x \sim 2$) [25]. Further studies by Ma *et al.* revealed the reduction of the pentoxide to NbO_2 and NbO post vacuum baking at 250°C for several hours [27]. These results are corroborated by the synchrotron measurements of Delheusy *et al.* [26] and ARXPS measurements by Dacca *et al.* [23]. Moreover, at the expense of dissolving the oxide, *in situ* vacuum baking drives inward oxygen diffusion from the oxide over the oxide/metal interface rather than into the vacuum [25, 26, 28–30]. Subsequent reoxidation studies *via* exposure to ambient air shows that a partially dissolved oxide grows at the oxide/metal interface and is morphologically equivalent to the native grown oxide without prior heat treatment [27].

In this paper, by investigating the role of vacuum baking on niobium SRF resonators that contain a ~ 5 nm full wet-grown native amorphous oxide, we find evidence that suggests that potentially magnetic niobium suboxides may serve as a source of TLS that limits the performance of 3-D Nb resonators and 2-D transmon qubits which utilize oxidized Nb. Modest *in situ* vacuum baking treatments (150 °C–200 °C) for durations as short as 25 minutes aggravate TLS-like losses that are eventually suppressed with increasing bake time. We recreate the *in situ* vacuum baking treatments within a time-of-flight secondary ion mass spectrometer (TOF-SIMS) on a Nb SRF resonator cutout and confirm that the oxide reduces considerably, suggesting the formation of possibly magnetic suboxides. We hypothesize that the non-monotonic evolution of Q_0 with successive baking is due to the interplay of TLS-hosting magnetic suboxide generation and oxide dissolution.

II. EXPERIMENTAL METHOD

For our studies, we used two 1.3 GHz TESLA-shaped [31] niobium single-cell SRF resonators that have undergone a bulk 120 μm removal from the inner RF surface *via* electropolishing, followed by 800 °C degassing, and an additional 40 μm removal from the inner surface *via* electropolishing [32]. The resonators were then exposed to air and high pressure rinsed with ultra-pure water,

forming a ~ 5 nm amorphous native oxide. Afterwards, the resonators were assembled for testing and evacuated to a vacuum level of approximately $1\text{E-}5$ Torr. Typically, resonators tested at this point are called electropolished (EP) resonators. The resonators then underwent sequential testing and treatment to various low temperature vacuum bakes [33] for increasing durations while actively pumping to maintain the vacuum level within the resonators. Such treatments have been shown to dissolve the native niobium oxide and introduce oxygen interstitial into the underlying niobium [25, 26, 28–30].

One resonator, TE1AES019, was first subjected to an *in situ* low temperature vacuum bake at 90 °C for 384 hours followed by sequential *in situ* baking steps at 200 °C for increasing durations. For the final treatment, the resonator was baked at 340 °C for 5 hours to ensure complete removal of the niobium pentoxide [10]. The resonator was RF tested after each step and maintained vacuum throughout the entire course of the study.

The second resonator, TE1AES021, was used to probe baking treatments that more closely resembled those typically utilized in transmon qubit fabrication and to better identify the source of additional RF loss. It underwent sequential *in situ* vacuum baking treatments at 150 °C with resonator RF measurements performed after each step. After the RF test post baking at 150 °C for a net duration of 15 hours and 25 minutes, resonator TE1AES021 was subjected to an *ex situ* vacuum bake at 200 °C for 19.5 hours. This involved first venting the resonator to atmosphere followed by vacuum baking. Afterwards, the resonator was once again high pressure rinsed, reforming the amorphous ~ 5 nm native oxide, but this time with a larger concentration of subsurface O interstitial present compared to the baseline measurement post EP. For the final treatment, the resonator underwent an HF acid rinse, which dissolved the native oxide, and upon subsequent high pressure rinsing, reformed a new native oxide at the expense of consuming approximately 2 nm of niobium [34].

To test our resonators, we utilized methods similar to those outlined in [9, 35]. Resonators were installed in large vertical helium dewars and cooled through the superconducting transition temperature at ~ 9.25 K while employing methods to minimize the possibility of trapping magnetic flux [36, 37]. Resonators were then driven at their resonant frequency while using a phase-locked loop to track and maintain resonance. We used a signal analyzer set to a resolution bandwidth of ~ 220 Hz to perform single shot, zero span decay measurements of the transmitted power $P_t(t)$ from the resonator after shutting off the incident RF power. By fitting the resulting $P_t(t)$ data with the procedure outlined in [9], we obtained a measure of Q_0 down to fields of $E_{acc} \sim 1$ kV/m with experimental error never exceeding 10 %. The fields were then converted into a measure of the photon number *via* $n = U/\hbar\omega$, where U is the stored energy in the resonator, which is related to $P_t(t)$. We performed the tests at temperatures of 1.4–1.6 K, where the population of

quasi-particles was virtually non-existent, and their contribution to the surface resistance was negligible. As a result, the quality factor in these tests was dominated by losses stemming from material properties. We note that while most TLS remain thermally saturated at these temperatures, there remains a small fraction of unsaturated TLS which drive the characteristic response of Q_0 with intra-resonator photon number [9, 10].

III. RESULTS

A. Resonator RF measurements

The upper panel in Fig. 1 presents data acquired on resonator TE1AES019 after an initial $90^\circ\text{C} \times 384$ hour *in situ* vacuum bake followed by sequential *in situ* vacuum bakes at various temperatures and durations. Shown also for reference is data from Romanenko and Schuster taken on an EP resonator which contains a full 5 nm native wet-grown oxide and serves as our baseline test [9]. For all tests, we observe the expected saturation of the quality factor at electric fields < 0.01 MV/m (i.e. photon numbers $< 2\text{E}18$) that is characteristic of two-level systems [6, 9, 10]. We find that the $90^\circ\text{C} \times 384$ hours + $200^\circ\text{C} \times 1$ hour *in situ* vacuum baking treatment produces a resonator with a low field quality factor of $9\text{E}9$, roughly three times lower than the baseline test. An additional $200^\circ\text{C} \times 5$ hour *in situ* vacuum bake produces identical results at fields below 0.1 MV/m. After a second round of $200^\circ\text{C} \times 5$ hour vacuum bake, a slight improvement in Q_0 up to $1.2\text{E}10$ occurs. For the final treatment, we subjected the resonator to a $340^\circ\text{C} \times 5$ hour vacuum baking treatment which is known to fully remove the native Nb_2O_5 layer [10, 38]. The resulting measurements display a Q_0 at low fields of greater than $7\text{E}10$, the highest achieved in this study, and in line with previous work [10, 38]. Overall, these tests show a non-monotonic dependence of resonator Q_0 with bake duration.

The lower panel in Fig. 1 depicts data taken on resonator TE1AES021 post various baking and chemical treatments. Surprisingly, we find that a modest *in situ* vacuum bake at 150°C for 25 minutes reduces the resonator Q_0 by a factor of two when compared to the baseline EP test from Romanenko and Schuster. Subjecting the resonator to an additional round of *in situ* vacuum baking at 150°C for 15 hours produces a low field Q_0 of $9\text{E}9$, identical to the results obtained on TE1AES019 after the first and second tests. The results post *ex situ* bake at 200°C for 19.5 hours, for which we re-iterate received subsequent high pressure rinsing with ultra-pure water, yield a Q_0 that is similar in value to the baseline EP at fields $< 4\text{E}-3$ MV/m. Subsequent HF acid rinsing and high pressure water rinsing reveals a Q_0 vs E_{acc} curve that is nearly identical to the baseline EP data.

We fit the data in Fig. 1 with the standard TLS model with a quasi-particle term built in. The electric field de-

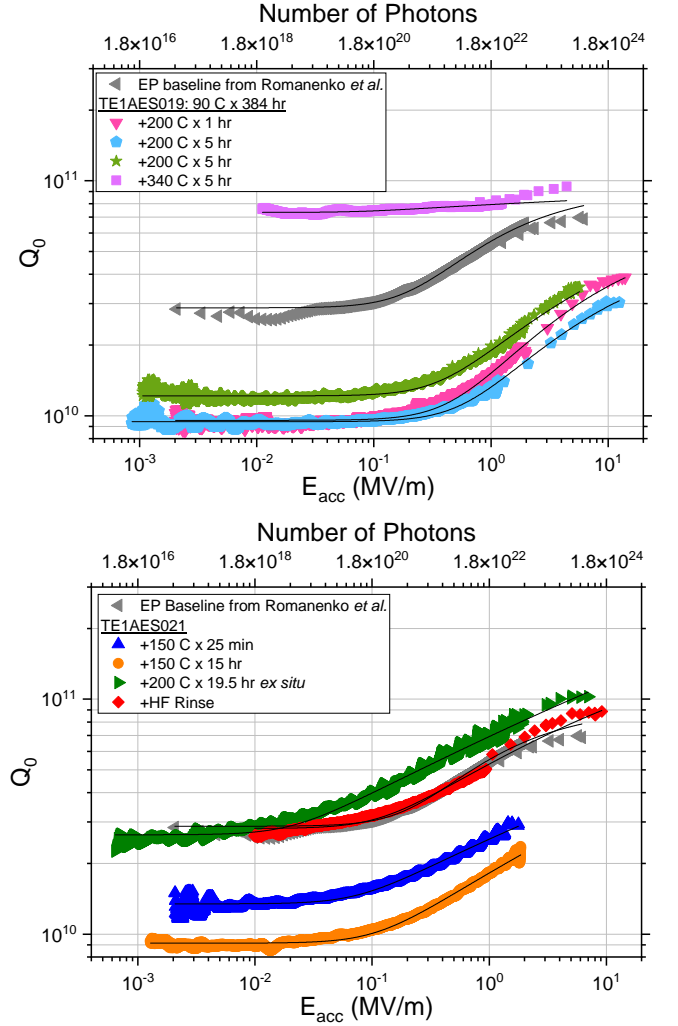


FIG. 1. Measurements of quality factor vs electric field at temperatures of 1.4 K-1.6 K for the 1.3 GHz 3-D Nb resonators TE1AES019 (upper) and TE1AES021 (lower) after sequential baking and chemical treatments. Upper axes plot the converted intra-resonator photon number. For reference, the gray left pointed triangles depict data obtained on an EP resonator which contained a full 5 nm native wet grown oxide from Romanenko and Schuster [9]. Solid black lines show fits with Eq. 2.

pendence of a niobium SRF resonator at low fields may be modelled as a single interface system (metal/air) containing TLS according to

$$\frac{1}{Q_0} = \frac{F\delta_0}{(1 + (\frac{E_{\text{acc}}}{E_c})^2)^\beta} + \frac{1}{Q_{qp}} \quad (2)$$

where β is a fitting parameter, E_c is the characteristic saturation field, δ_0 is the dielectric loss, and Q_{qp} is the quasi-particle contribution to RF loss [9, 13]. Fig. 2 plots the product of the filling factor and dielectric loss tangent for each curve presented in Fig. 1. We choose to present this convolved product as it is agnostic to the precise val-

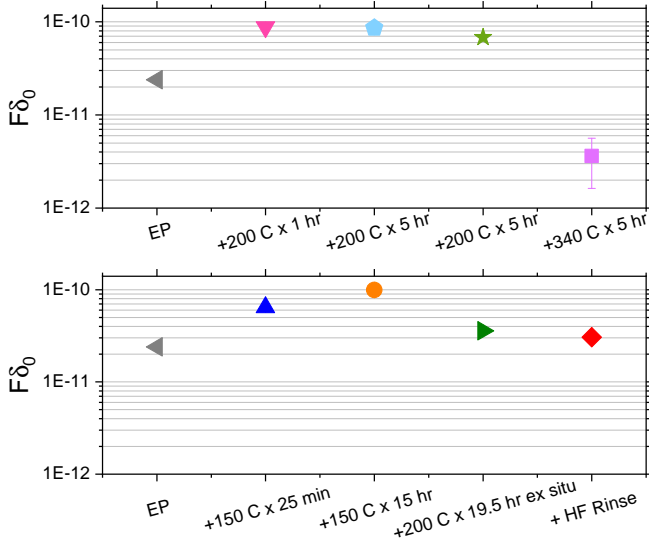


FIG. 2. Fitted $F\delta_0$ values and fit error of TE1AES019 (upper) and TE1AES021 (lower) using the data presented in Fig. 1. The $90^\circ\text{C} \times 384$ hours *in situ* vacuum bake that precedes the sequential *in situ* vacuum baking treatments for resonator TE1AES019 has been omitted from the horizontal axis for brevity. Most error bars are smaller than the symbol size.

ues of the filling factor and loss tangent and gives a qualitative measure of the TLS contribution to RF loss. Resonator TE1AES019 shown in the upper panel of Fig. 2 displays a non-monotonic dependence of the TLS-driven losses with *in situ* vacuum baking, achieving as low as $3.63\text{E-}12$ after the final round of treatment, consistent with previous results [10]. TE1AES021 presented in the lower panel suggests that while *in situ* vacuum baking increases TLS-driven RF losses, treatments which utilize high pressure water rinsing returns them to the baseline EP values.

B. TOF-SIMS studies

As the amorphous niobium oxide is known to be a host of TLS, it is likely that its dynamics dictate the performance evolution observed in Figs. 1 and 2. To investigate this possibility, we studied the effect of sequential vacuum baking at 205°C on an electropolished niobium SRF resonator cutout in a time-of-flight secondary ion mass spectrometer (TOF-SIMS). We used a liquid bismuth ion Bi^+ beam to perform secondary ion mass measurements while sputtering with a 1 keV cesium ion Cs^+ gun to obtain depth profiles of the oxide. The sample was sequentially vacuum baked in steps of 205°C *in situ* followed by cool down to and measurement at room temperature. Two depth profiles were obtained at different spots on the sample after each step of treatment. All measurements were performed in a vacuum better than $1\text{E-}10$ Torr. Fig. 3 presents the resulting averaged Nb_2O_5^- data.

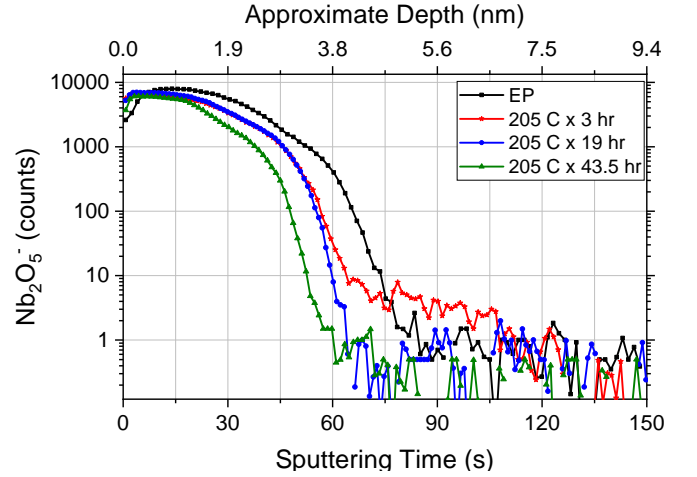


FIG. 3. TOF-SIMS depth profiles of the Nb_2O_5^- signal acquired on an as-received electropolished resonator cutout subjected to sequential rounds of *in situ* vacuum baking. Durations presented in the legend represent integrated bake times.

The as-received electropolished resonator cutout, which is denoted as “EP” in Fig. 3, displays a fully intact 5 nm native pentoxide. After the first round of *in situ* baking at 205°C for 3 hours, we find that this Nb_2O_5^- layer is reduced slightly. In addition, there is an anomalous tail which begins at a depth of 4.1 nm and extends further toward the bulk. After baking the sample for a total of 19 hours, we find a nearly identical Nb_2O_5^- signal compared to the preceding treatment but without the presence of the anomalous tail. Baking for a net duration of 43.5 hours shows a further reduction in the thickness of the Nb_2O_5^- layer.

The evolution of the SIMS profiles presented in Fig. 3 confirms the gradual dissolution of the native Nb_2O_5 layer with sequential *in situ* vacuum baking at 205°C . This confirms the observations of previous works and suggests that this dissolution is accompanied by the growth of the NbO_2 and NbO suboxides [23–27] as well as the inward diffusion of oxygen over the oxide/metal interface [25, 26, 28–30].

IV. DISCUSSION

The prominent increase in TLS-driven losses combined with the reduction in Nb_2O_5 and subsequent growth of suboxides after *in situ* baking at 205°C or 150°C suggests the role of niobium suboxides as a source of TLS. Indeed, previous tunneling and XPS measurements on cavity-grade niobium baked at various temperatures and durations show that, when compared to an unbaked niobium sample, the $250^\circ\text{C} \times 2$ hr bake not only causes Nb_2O_5 to reduce into its suboxides but also yields an increased level of subgap states which is likely driven by magnetic moments formed due to the presence of oxygen vacancies within the oxide [17]. Moreover, other

work has shown that these magnetic moments increase with oxygen vacancy concentration [16]. As such, *in situ* vacuum baking may promote the growth of magnetic suboxides that drive TLS-like losses in 3-D niobium resonators. The aggravation and subsequent mitigation of TLS-driven losses post *in situ* vacuum baking is likely due to the interplay of magnetic suboxide generation and oxide dissolution.

This hypothesis is further corroborated by the fact that treatments which re-expose the resonator to air and reform the native oxide show nearly identical TLS-driven losses when compared to the baseline EP test. Moreover, despite the fact that TE1AES021 post the additional HF acid rinse contained a larger concentration of interstitial oxygen in the underlying niobium material, it gave nearly identical performance to the test post baseline EP in Figs. 1 and 2. This localizes the TLS losses to the oxide and asserts the non-role of interstitial oxygen in niobium. This further supports the conclusions made in [9].

We note that while TE1AES021 post the additional 200 °C for 19.5 hour *ex situ* bake yields similar results to the baseline EP test, they vary slightly. Previous work suggests that a partially dissolved oxide readily forms a new oxide upon re-oxidation that is morphologically identical to the native grown oxide without an intermediate heat treatment [27]. However, our results suggest there may exist some minute variations at the interface which may drive the differing RF performance. This will be a subject of future study.

Fig. 4 presents the additional surface resistance due to TLS-induced dissipation for resonator TE1AES019 post the 90 °C \times 384 hours + 200 °C \times 1 hour vacuum baking treatment. This was obtained using the relation $R_s = G/Q_0$ (G is a known geometry factor) and by subtracting off the contribution from non-TLS losses. Surprisingly, the surface resistance at low fields levels off at 22.5 n Ω , roughly two times larger than what was reported for a 100 nm thick niobium oxide grown *via* anodization [9]. This is also well explained by the magnetic suboxide hypothesis as oxides grown through anodization are known to contain fewer oxygen vacancies than wet grown oxides [39]. As a result, while the partially depleted oxide post vacuum baking is significantly thinner than 100 nm, it may host a larger concentration of magnetic moments within the suboxides and thus introduce a greater level of TLS losses.

While the present work focuses on the effect of vac-

uum baking on 3-D niobium SRF resonator performance in the quantum regime, the observations made here are applicable to transmon qubits which utilize oxidized niobium. As many qubit fabrication processes perform vacuum baking treatments after the deposition and oxidation of niobium thin films, there exists the potential of generating additional magnetic suboxides which may further limit transmon qubit quantum coherence times.

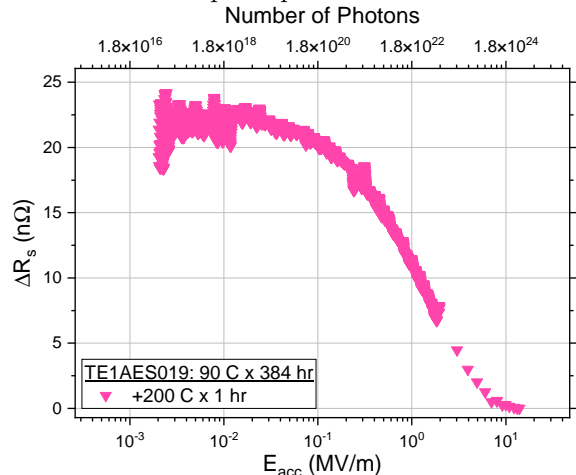


FIG. 4. Surface resistance introduced by TLS for resonator TE1AES019 post 90 °C \times 384 hour + 200 °C \times 1 hour shown in the upper panel in Fig. 1.

V. CONCLUSION

In summary, we studied the effect of low temperature vacuum baking on the quality factor of two 1.3 GHz 3-D niobium SRF resonators and found evidence which suggests that magnetic suboxides are a potential source of TLS losses that limit performance in both Nb resonators and transmon qubits which utilize oxidized Nb. *In situ* vacuum baking produces an aggravation and subsequent mitigation of these losses due to the interplay of magnetic suboxide generation and oxide dissolution.

VI. ACKNOWLEDGMENTS

This material is based upon work supported by the U.S. Department of Energy, Office of Science, National Quantum Information Science Research Centers, Superconducting Quantum Materials and Systems Center (SQMS) under contract number DE-AC02-07CH11359.

-
- [1] J. Clarke and F. Wilhelm, Superconducting quantum bits, *Nature* **453**, 1031 (2008).
 - [2] S. E. de Graaf, L. Faoro, L. B. Ioffe, S. Mahashabde, J. J. Burnett, T. Lindström, S. E. Kubatkin, A. V. Danilov, and A. Y. Tzalenchuk, Two-level systems in supercon-

ducting quantum devices due to trapped quasiparticles, *Sci. Adv.* **6** (2020).

- [3] P. De Visser, D. Goldie, P. Diener, S. Withington, J. Baselmans, and T. Klapwijk, Evidence of a nonequilibrium distribution of quasiparticles in the microwave re-

- sponse of a superconducting aluminum resonator, *Phys. Rev. Lett.* **112**, 047004 (2014).
- [4] A. P. Vepsäläinen, A. H. Karamlou, J. L. Orrell, A. S. Dogra, B. Loer, F. Vasconcelos, D. K. Kim, A. J. Melville, B. M. Niedzielski, J. L. Yoder, and et al., Impact of ionizing radiation on superconducting qubit coherence, *Nature* **584**, 551–556 (2020).
 - [5] J. M. Martinis, Saving superconducting quantum processors from decay and correlated errors generated by gamma and cosmic rays, *Npj Quantum Inf.* **7**, 90 (2021).
 - [6] D. P. Pappas, M. R. Vissers, D. S. Wisbey, J. S. Kline, and J. Gao, Two level system loss in superconducting microwave resonators, *IEEE Trans. on Appl. Supercond.* **21**, 871 (2011).
 - [7] C. Wang, C. Axline, Y. Y. Gao, T. Brecht, Y. Chu, L. Frunzio, M. H. Devoret, and R. J. Schoelkopf, Surface participation and dielectric loss in superconducting qubits, *Appl. Phys. Lett.* **107**, 162601 (2015).
 - [8] W. Woods, G. Calusine, A. Melville, A. Sevi, E. Golden, D. Kim, D. Rosenberg, J. Yoder, and W. Oliver, Determining interface dielectric losses in superconducting coplanar-waveguide resonators, *Phys. Rev. Appl.* **12**, 014012 (2019).
 - [9] A. Romanenko and D. I. Schuster, Understanding quality factor degradation in superconducting niobium cavities at low microwave field amplitudes, *Phys. Rev. Lett.* **119**, 264801 (2017).
 - [10] A. Romanenko, R. Pilipenko, S. Zorzetti, D. Frolov, M. Awida, S. Belomestnykh, S. Posen, and A. Grassellino, Three-dimensional superconducting resonators at 20 mk with photon lifetimes up to $\tau = 2$ s, *Phys. Rev. Appl.* **13**, 034032 (2020).
 - [11] M. Reagor, H. Paik, G. Catelani, L. Sun, C. Axline, E. Holland, I. M. Pop, N. A. Masluk, T. Brecht, L. Frunzio, M. H. Devoret, L. Glazman, and R. J. Schoelkopf, Reaching 10 ms single photon lifetimes for superconducting aluminum cavities, *Appl. Phys. Lett.* **102**, 192604 (2013).
 - [12] P. W. Anderson, B. I. Halperin, and c. M. Varma, Anomalous low-temperature thermal properties of glasses and spin glasses, *Philos. Mag.* **25**, 1 (1972).
 - [13] J. M. Martinis, K. B. Cooper, R. McDermott, M. Steffen, M. Ansmann, K. D. Osborn, K. Cicak, S. Oh, D. P. Pappas, R. W. Simmonds, and C. C. Yu, Decoherence in josephson qubits from dielectric loss, *Phys. Rev. Lett.* **95**, 210503 (2005).
 - [14] J. Verjauw, A. Potočník, M. Mongillo, R. Acharya, F. Mohiyaddin, G. Simion, A. Pacco, T. Ivanov, D. Wan, A. Vanleenhove, L. Souriau, J. Jussot, A. Thiam, J. Swerts, X. Piao, S. Couet, M. Heyns, B. Govoreanu, and I. Radu, Investigation of microwave loss induced by oxide regrowth in high-Q niobium resonators, *Phys. Rev. Appl.* **16**, 014018 (2021).
 - [15] M. V. P. Altoé, A. Banerjee, C. Berk, A. Hajr, A. Schwartzberg, C. Song, M. Alghadeer, S. Aloni, M. J. Elowson, J. M. Kreikebaum, E. K. Wong, S. M. Griffin, S. Rao, A. Weber-Bargioni, A. M. Minor, D. I. Santiago, S. Cabrini, I. Siddiqi, and D. F. Ogletree, Localization and mitigation of loss in niobium superconducting circuits, *PRX Quantum* **3**, 020312 (2022).
 - [16] R. J. Cava, B. Batlogg, J. J. Krajewski, H. F. Poulsen, P. Gammel, W. F. Peck, and L. W. Rupp, Electrical and magnetic properties of $\text{Nb}_2\text{O}_{5-\delta}$ crystallographic shear structures, *Phys. Rev. B* **44**, 6973 (1991).
 - [17] T. Proslir, J. Zasadzinski, L. Cooley, M. Pellin, J. Norem, J. Elam, C. Z. Antoine, R. A. Rimmer, and P. Kneisel, Tunneling study of SRF cavity-grade niobium, *IEEE Trans. on Appl. Supercond.* **19**, 1404 (2009).
 - [18] T. F. Harrelson, E. Sheridan, E. Kennedy, J. Vinson, A. T. N'Diaye, M. V. P. Altoé, A. Schwartzberg, I. Siddiqi, D. F. Ogletree, M. C. Scott, and S. M. Griffin, Elucidating the local atomic and electronic structure of amorphous oxidized superconducting niobium films, *Appl. Phys. Lett.* **119**, 244004 (2021).
 - [19] E. Sheridan, T. F. Harrelson, E. Sivonxay, K. A. Persson, M. V. P. Altoé, I. Siddiqi, D. F. Ogletree, D. I. Santiago, and S. M. Griffin, Microscopic theory of magnetic disorder-induced decoherence in superconducting Nb films (2021).
 - [20] C. Müller, J. H. Cole, and J. Lisenfeld, Towards understanding two-level-systems in amorphous solids: insights from quantum circuits, *Rep. on Prog. Phys.* **82**, 124501 (2019).
 - [21] J. Halbritter, On the oxidation and on the superconductivity of niobium, *Appl. Phys. A* **43**, 1 (1987).
 - [22] Y. Zhao, Z. Zhang, and Y. Lin, Optical and dielectric properties of a nanostructured NbO_2 thin film prepared by thermal oxidation, *J. Phys. D* **37**, 3392 (2004).
 - [23] A. Daccà, G. Gemme, L. Mattera, and R. Parodi, XPS analysis of the surface composition of niobium for superconducting RF cavities, *Appl. Surf. Sci.* **126**, 219 (1998).
 - [24] B. King, H. Patel, D. Gulino, and B. Tatarchuk, Kinetic measurements of oxygen dissolution into niobium substrates: In situ x-ray photoelectron spectroscopy studies, *Thin Solid Films* **192**, 351 (1990).
 - [25] Q. Ma, P. Ryan, J. W. Freeland, and R. A. Rosenberg, Thermal effect on the oxides on Nb(100) studied by synchrotron-radiation x-ray photoelectron spectroscopy, *J. Appl. Phys.* **96**, 7675 (2004).
 - [26] M. Delheusy, A. Stierle, N. Kasper, R. P. Kurta, A. Vlad, H. Dosch, C. Antoine, A. Resta, E. Lundgren, and J. Andersen, X-ray investigation of subsurface interstitial oxygen at Nb/oxide interfaces, *Appl. Phys. Lett.* **92**, 101911 (2008).
 - [27] Q. Ma and R. A. Rosenberg, Angle-resolved x-ray photoelectron spectroscopy study of the oxides on Nb surfaces for superconducting RF cavity applications, *Appl. Surf. Sci.* **206**, 209 (2003).
 - [28] K. Schulze and H. Jehn, Sauerstofflöslichkeit in niob im stationären zustand, *Z. Metallkd.* **68** (1977).
 - [29] E. Fromm and E. Gebhardt, Gase und kohlenstoff in metallen. Reine und angewandte metallkunde in einzeldarstellungen, *Berichte der Bunsengesellschaft für physikalische Chemie* **81**, 777 (1977).
 - [30] E. M. Lechner, J. W. Angle, F. A. Stevie, M. J. Kelley, C. E. Reece, and A. D. Palczewski, RF surface resistance tuning of superconducting niobium via thermal diffusion of native oxide, *Appl. Phys. Lett.* **119**, 082601 (2021).
 - [31] B. Aune *et al.*, Superconducting tesla cavities, *Phys. Rev. ST Accel. Beams* **3**, 092001 (2000).
 - [32] H. Padamsee, J. Knobloch, and T. Hays, *RF Superconductivity for Accelerators* (Wiley-VCH Verlag GmbH and Co., KGaA, Weinheim, 1998).
 - [33] H. Padamsee, *RF Superconductivity: Volume II: Science, Technology and Applications* (Wiley-VCH Verlag GmbH and Co., KGaA, Weinheim, 2009).
 - [34] M. Checchin and A. Grassellino, High-field Q-slope mitigation due to impurity profile in superconducting radio-

- frequency cavities, *Appl. Phys. Lett.* **117**, 032601 (2020).
- [35] O. Melnychuk, A. Grassellino, and A. Romanenko, Error analysis for intrinsic quality factor measurement in superconducting radio frequency resonators, *Rev. Sci. Instrum.* **85**, 124705 (2014).
 - [36] A. Romanenko, A. Grassellino, O. Melnychuk, and D. A. Sergatskov, Dependence of the residual surface resistance of superconducting radio frequency cavities on the cooling dynamics around T_c , *J. of Appl. Phys.* **115**, 184903 (2014).
 - [37] S. Posen, M. Checchin, A. C. Crawford, A. Grassellino, M. Martinello, O. S. Melnychuk, A. Romanenko, D. A. Sergatskov, and Y. Trenikhina, Efficient expulsion of magnetic flux in superconducting radiofrequency cavities for high Q_0 applications, *J. of Appl. Phys.* **119**, 213903 (2016).
 - [38] S. Posen, A. Romanenko, A. Grassellino, O. Melnychuk, and D. Sergatskov, Ultralow surface resistance via vacuum heat treatment of superconducting radio-frequency cavities, *Phys. Rev. Appl.* **13**, 014024 (2020).
 - [39] M. Grundner and J. Halbritter, XPS and AES studies on oxide growth and oxide coatings on niobium, *J. Appl. Phys.* **51**, 397 (1980).